

# Caustics and clustering in the vicinity of a vortex

S. Ravichandran and Rama Govindarajan  
*TIFR Centre for Interdisciplinary Sciences*  
*Tata Institute of Fundamental Research,*  
*Narsingi, Hyderabad, 500075, India.*  
*ravis@tifrh.res.in, rama@tifrh.res.in.*

We study the formation of caustics in vortex-dominated flows. We find that only particles starting within a critical distance of a vortex which scales as the square roots of the particle inertia and the circulation can form sling caustics. We show that particles starting in an annular region around this critical radius contribute the densest clusters in the flow. The large density spikes occurring for such particles, even at small inertia, are indicative that these particles will experience large collision rates.

## I. INTRODUCTION

When a turbulent flow contains small particles of a different density dispersed in it, these particles tend to cluster into small regions of the flow rather than being homogeneously distributed in space [1–5]. Several different but related ways of explaining this clustering have been posited [6–9]. Typically, heavy particles are centrifuged out of vortical regions and cluster into regions of high strain [10]. This effect can be observed for particles that are larger (typical of laboratory studies, see e.g. [4]) or smaller than the Kolmogorov scale. In particular, the behaviour of heavy particles much smaller than the Kolmogorov scale can be described using a simple equation (see eq. (1)) and is important in atmospheric flows.

Particle inertia also leads to the formation of caustics. At a given time instant, the velocities of two neighboring particles can differ greatly from each other. Velocity contours of inertial particles may thus display discontinuities and multi-valuedness in some regions of the flow. Such regions are known as caustics, where particle velocity may not be described as a single-valued field. The effects of caustics have been extensively studied [11–19]. For example Mehlig and Wilkinson [11] describe caustics as occurring due to folds in the velocity in phase space, leading to points in space where there are multiple values for the velocity at the same instant of time. Falkovich *et al.* [20] describe the same phenomenon as the formation of caustics due to the ‘sling effect’ or centrifugal action near the vortices. Caustics increase the collision rates for particles drastically, and have been suggested as a mechanism for the suddenness of the onset of rain in convecting cumulus clouds [11, 13, 20].

We ask how important the processes of sling caustics and preferential concentration are relative to each other. To this end we examine the archetypal flow for the sling effect: the flow due to a point vortex. In the process of being centrifuged out of vortical regions, particles which are closer to a vortex attain higher acceleration, and can eventually catch up with, or even overtake, particles which were initially further away from the vortex, thus forming caustics. We show that caustic-formation is only possible for particles initially located within a critical distance  $r_{cr} \simeq 1/2\sqrt{\Gamma\tau}$  of a point vortex, where  $\Gamma$  is the circulation of the vortex and  $\tau$  is the relaxation time of the particles, such that the particle Stokes number at the critical radius,  $St = \Gamma\tau/r_{cr}^2$ , is of order 1. Interestingly we find that the largest contributions to clustering come from the band of particles located in an annular region around this critical radius. This has consequences both for collision of particles and for condensation inhomogeneities.

We note that the system of particles around a vortex has been studied previously by Raju & Meiburg[21]. They provide a detailed discussion of the different particle-inertia regimes involved, and find similar spikes in density as we report in section III. They also report an increased ‘‘accumulation rate’’ for intermediate values of the particle Stokes number. Their work was done before the idea of inertial particle caustics came about, and we find that caustics provide a way of understanding their results.

In section II, we discuss the general nature of the problem, including the different possible initial conditions that can be used. In section III, we look at point vortices in particular. We discuss when caustics can form in the flow around a vortex, and show some scaling laws that are obeyed. Since point vortices are idealisations and viscosity smears them out, we examine caustics formation due to Gaussian vortices in IV. In section V, we report simulations with many vortices in a doubly-periodic box. We conclude in section VI.

## II. CAUSTICS AROUND A VORTEX

We prescribe a two-dimensional steady axisymmetric flow field, with its centre at the origin of the coordinate system. The radius  $a$  of the particle is taken to be much smaller than the typical flow length scales. The motion of

such an inertial particle in a flow field  $\mathbf{u}(\mathbf{x}, t)$  is given by the Maxey-Riley equations [22]. For particles much smaller than the Kolmogorov scale, and much denser than the fluid, the Maxey-Riley equations simplify to

$$\begin{aligned}\frac{d\mathbf{r}}{dt} &= \mathbf{v} \\ \frac{d\mathbf{v}}{dt} &= \frac{\mathbf{u} - \mathbf{v}}{\tau},\end{aligned}\tag{1}$$

where  $\mathbf{r}$  and  $\mathbf{v}$  are the particle location and velocity respectively, and  $t$  is time. The effect of particle inertia is encapsulated in the particle time-lag  $\tau$ .

The most general axisymmetric flow field is given by

$$\Omega \sim \frac{1}{r^p} \quad \text{or} \quad |\mathbf{u}| = r\Omega \sim r^{1-p},\tag{2}$$

where  $\Omega(r)$  is the angular velocity of a fluid particle at a radius  $r$ . For solid body rotation,  $p = 0$ , whereas for a flow with a single point vortex placed at the origin,  $p = 2$ . In cylindrical polar  $(r, \theta)$  coordinates equation (1) is written, with

$$\omega \equiv d\theta/dt,\tag{3}$$

as

$$\begin{aligned}\dot{r} &= v_r \\ \dot{v}_r + \frac{v_r}{\tau} &= r\omega^2 \\ (r^2\dot{\omega}) + \frac{r^2\omega}{\tau} &= \frac{r^2\Omega}{\tau}.\end{aligned}\tag{4}$$

where the dot superscript stands for  $d(\cdot)/dt$ . Particle dynamics in the vicinity of one vortex has been studied using the above equations in some detail by Raju & Meiburg [21] and by Shaw *et al.* [5].

From these solutions it is known that the radial distance of a particle from the center of the coordinate system is a monotonically increasing function of time. At long times the tangential velocity of a particle will approach that of the fluid, i.e.,  $\omega \simeq \Omega$  and so from equation (4), we have at long time or large radial distance,  $v_r \simeq \tau r \Omega^2$  and the particle's radial acceleration is negligible.

We prescribe two rings of particles at initial radii  $r_{01}$  and  $r_{02}$  with initial angular velocities  $\omega_i = \omega_0(r_i)$ ,  $i = 1, 2$ . Equations (4) then give

$$\begin{aligned}\frac{d\Delta r}{dt} &= \Delta v_r \\ \frac{d\Delta v_r}{dt} + \frac{\Delta v_r}{\tau} &= \Delta(r\omega^2) \\ \frac{d}{dt}\Delta(r^2\omega) + \frac{\Delta(r^2\omega)}{\tau} &= \frac{\Delta(r^2\Omega)}{\tau}\end{aligned}\tag{5}$$

where  $\Delta(\cdot) = (\cdot)_2 - (\cdot)_1$  represents a difference in a given quantity between the two rings of particles. In the following we define  $\Delta r_0 \equiv \Delta r(t = 0)$  and use the shorthand notation  $r_0$  for the initial location  $r_{01}$  of the inner ring.

A caustic can be said to have formed if, at a particular finite time  $t$ , particles on both rings arrive the same radius  $r$  but with different velocities, i.e. if  $\Delta r = 0$ , but  $\Delta v_r \neq 0$ . Note in particular that particles which asymptotically approach each other at long times do not give rise to caustics, although they do contribute to clustering. When a caustic occurs, trajectories in the phase portrait for the relative position and velocity look like the curve 'b' in figure 1 and not like curve 'a'.

We can solve the system (5) for the general vortex  $\Omega \sim r^{-p}$  and plot the separatrix in  $r_0 - \Delta r$  space between caustic-forming and no-caustic regimes. We only show results for  $p = 2$ , and comment on the implications of  $p \neq 2$  (see end of section IV).

We use three kinds of initial conditions for this study. The first, one we shall call co-rotating (or 'zero-inertia'), that the particles follow the flow exactly until  $t = 0$ , and particle inertia is switched on at  $t = 0$ . For particles of small inertia this is a reasonable condition [21]. In the second initial condition, particles are initially motionless and the vortex is introduced at  $t = 0$ . We shall refer to this as the zero-velocity initial condition. A turbulent patch moving into a particle-rich region would correspond to this situation. Most studies of particles in turbulence employ one of

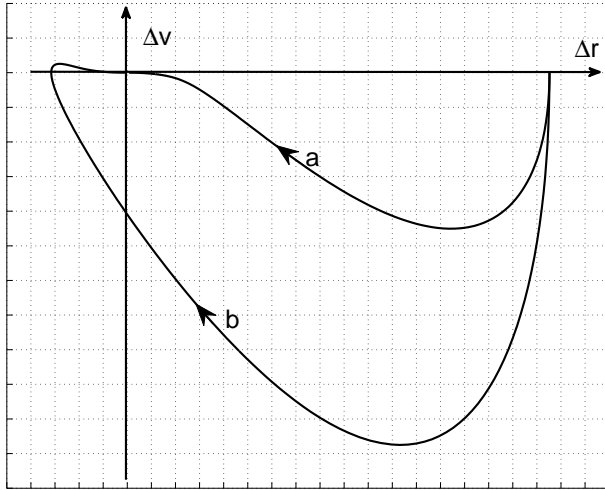


Figure 1: Schematic of possible trajectories for the system (5). At long times, the two rings of particles will come closer to each other and merge at infinite time, and this would, in the absence of caustics, give rise to a trajectory of type (a). In the caustics forming case, the ring closer to the origin at initial time would catch up with and overtake the ring further out, so the relative velocity would cross zero once in finite time, as in trajectory (b).

these two conditions. Also consider a vortex tube being stretched by the turbulent flow around it. The strength of the vortex will grow with time until it reaches its maximum value. To mimic this situation, a third initial condition, which is just a generalisation of the second, is where both particles and vortex are initially motionless, and the strength of the vortex is gradually ramped up to its final value. The results from this third initial condition are not presented here because they display no unexpected physics. The introduction of another time scale of growing vorticity merely scales the answers appropriately. Most real-life situations will correspond with reasonable fidelity to one of our initial conditions or something in-between, so we expect our results to have a bearing on understanding clustering.

The time and length scales inherent to the problem respectively are the inertial timescale  $\tau$  of the particle and  $L = \sqrt{\Gamma\tau}$  where  $\Gamma$  is the strength of the vortex. Note that  $\Gamma$  and  $\tau$  are the only parameters in the problem. For a given initial condition, from dimensional arguments we may argue that the caustic-formation time  $T_{caustic}$  will have to depend on nondimensional groups formed out of the scales of the problem, and must have a functional form

$$\frac{T_{caustic}}{\tau} = T\left(\frac{r_0}{\sqrt{\Gamma\tau}}, \frac{\Delta r}{\sqrt{\Gamma\tau}}\right). \quad (6)$$

If there is indeed a regime where it is impossible for caustics to form, the caustic-formation time must diverge in this regime. We may then define a critical initial separation  $\Delta r_{cr}$ , as the maximum value of the initial separation for a given  $r_0$  up to which caustics can occur. This quantity, suitably scaled, will be a function only of the initial distance from the centre of the vortex, i.e.,

$$\frac{\Delta r_{cr}}{\sqrt{\Gamma\tau}} = f\left(\frac{r_0}{\sqrt{\Gamma\tau}}\right). \quad (7)$$

We study in detail the case of a single point vortex, and then examine the case of Gaussian vortices. Finally we will derive a necessary condition for caustics formation for a general axisymmetric flow.

### III. POINT VORTEX

For a point vortex, we substitute  $p = 2$  in equation (2). The flow field is now given by

$$\mathbf{u} = \frac{\Gamma}{2\pi r} \mathbf{e}_\theta.$$

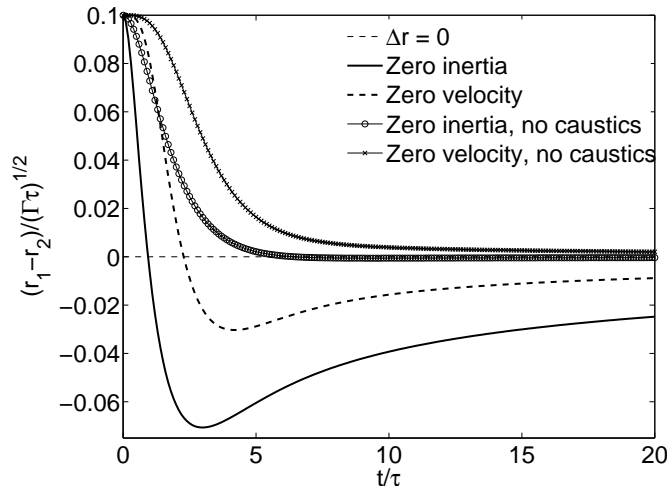


Figure 2: The separation between particle-pairs as a function of time, illustrating the difference between the types of initial conditions. The curves that do or do not cut the  $\Delta r = 0$  axis are respectively for particles that do or do not form caustics. Note that a maximum of one crossing of the  $\Delta r = 0$  line can occur for a given curve.

Using  $\tau$  and  $\sqrt{\Gamma\tau}$  as scales, equations 4 may be written in non-dimensional form as

$$\ddot{x} + \dot{x} = \frac{\zeta^2}{x^3} \quad (8)$$

$$\text{and} \quad \dot{\zeta} + \zeta = 1, \quad (9)$$

where  $x = r/(\tau\Gamma)^{1/2}$  and  $\zeta \equiv r^2\omega/\Gamma$ . We note that these equations are independent of  $\tau$ , i.e., the existence of caustics can be investigated with the particle size scaled out. From equation (9) it is clear that the azimuthal motion merely relaxes from any initial condition to  $\zeta = 1$  on a time-scale of  $\tau$ . At longer times, and when  $x \gg 1$ , irrespective of the initial condition, equation (8) thus reduces to one where  $\ddot{x}$  is negligible and  $\dot{x} \sim f(x)$ . In such a regime, given that  $v_r > 0$  (because of the centrifugal nature of particle motion), it is obvious that two particles which are at different radii at a given time  $t$  in this regime will never produce a caustic. It follows that only particles which start out at small radial distance will accelerate enough to form caustics.

A numerical solution of equation (8) enables us to divide the parameter space into regimes where caustics formation is possible and regimes where it is not. Figure 2 shows examples of both of these, and how the separation between the two rings of particles progresses with time.

### A. Limits for caustics formation

The time at which each curve crosses the  $\Delta r = 0$  line is  $T_{caustic}$ . We expect the caustic-formation time to be small for small initial separations of the two rings of particles, and plot this quantity for  $\Delta r_0 = 10^{-4}$  in figure 3. It is immediately clear that the caustic-formation time diverges even for this small separation above an  $x_0$  of about 0.5, for both initial conditions. We define the initial radius of the inner ring, above which caustics cannot form, as  $r_{cr}$ . In the region where  $r_0 < r_{cr}$ , we see that  $T_{caustic}$  scales as  $r_0^2$  for the zero inertia initial condition, and as  $r_0$  for the zero velocity initial condition. Note that, for the zero inertia initial condition,  $T_{caustic}$  is seemingly independent of  $\tau$ , since  $T_{caustic}/\tau$  scales as  $(r_0)^2/(\Gamma\tau)$ . After Raju & Meiburg[21], we can argue for this condition that the initial velocity term in equation 8 is negligible. This gives an equation for the evolution at early times of the separation between particles that goes as (assuming  $\Delta r \ll r_0$ ):

$$\frac{d^2}{dt^2} \Delta r \sim \frac{\Delta r}{r_0^4}.$$

This suggests that  $T_{caustics}$  should scale as  $r_0^2$  for a given  $\Delta r$ . For the zero velocity initial condition, this simplification is not possible, and we can think of no simple argument at this point for the scaling as  $St^{-1/2}$ .

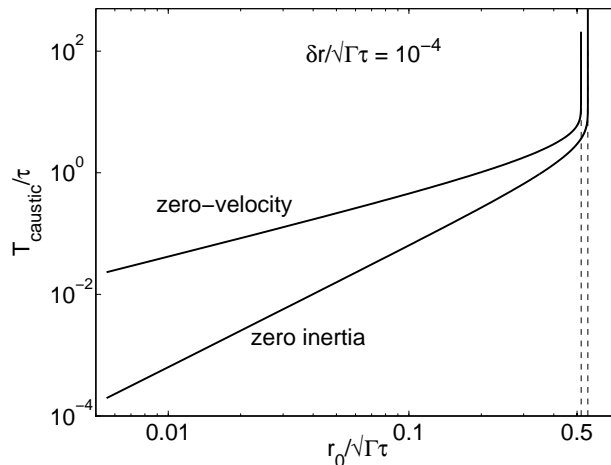


Figure 3: The caustic-formation time  $T_{caustic}$  as a function of the initial location of the inner ring of particles. A very small separation between the rings is used in this case, and the location of divergence is insensitive to further reduction in separation.

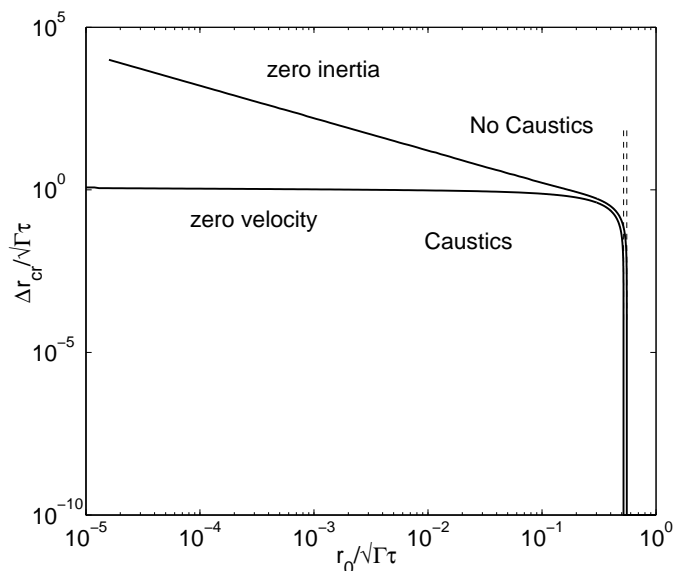


Figure 4: Maximum initial separation for caustics formation for the zero-inertia and the zero-velocity initial conditions. Caustics can occur below or to the left of the lines. The curves for different  $\tau$  collapse onto each other when they are scaled according to equation 7. For the zero-inertia initial condition,  $r_0$  and  $\Delta r_{cr}$  are inversely related.

Figure 4 shows the maximum initial separation  $(\Delta r)_{cr}$  for caustics to occur, as a function of  $r_0$ . It is evident that beyond a certain  $r_0 = r_{cr}$ , however small the initial separation, caustics cannot occur. For initial particle locations within a critical radius, one may have caustics, created with particles which are located within a certain critical separation distance  $(\Delta r)_{cr}$ . This quantity depends on the initial condition. For a range of  $r_0$ , with initially co-rotating particles, the initial radius and the maximum separation for caustics obey an inverse relationship, i.e.  $r_0(\Delta r)_{cr}/(\Gamma\tau)$  is constant. The zero-velocity initial condition, on the other hand, yields a much lower  $\Delta r_{cr}$  which varies much more slowly with  $r_0$ .

If the inverse relationship of  $(\Delta r)_{cr}$  and  $r_0$  is combined with the scaling argument for  $T_{caustic}$ , we can obtain a scaling for a "critical" velocity  $(\Delta r)_{cr}/T_{caustic} \sim \Gamma^2\tau/r_0^3$ . Comparing this with equation (4) suggests that the particles that bridge the largest gaps move outwards almost ballistically and the acceleration term is unimportant for such particles.

## B. Particle density

We know that inertial particles in a vortical flow cluster into regions of high density. We would like to understand the role of sling caustics in this process. We track the density of inertial particles using the Lagrangian particle tracking method of Osipov following Healy & Young [23]. This approach has been used in the past (see [24, 25]). The equations are given in the appendix. By this approach, one may track the density in the vicinity of a given particle while moving with the particle. The method relies on keeping track of the net divergence of particle velocities in this moving vicinity. The Osipov method allows for obtaining local densities without actually tracking many rings of particles. Figure 5 (a) shows density profiles as functions of time in the vicinity of particles started at different  $r_0$ . Densities in the vicinity of particles whose initial locations lie within  $r_{cr}$ , i.e., those which can participate in caustics formation, are shown by dashed lines, whereas for particles starting out at  $r_0 > r_{cr}$ , i.e., in regions which do not allow caustics, local densities are shown by solid lines. The difference between the two is stark. Outside the regime that allows caustics, all that happens is that particles cluster slowly with time, and the (Lagrangian) density monotonically increases. On the other hand, densities of particles starting from within the regime of caustics formation show a sharp spike around  $t = T_{caustic}$  for that  $r_0$ , and subsequently the Lagrangian density decreases monotonically, since particles which participate in caustics formation later display trajectories that diverge in radius. The spikes happen by virtue of a patch of particles that start out within a small neighbourhood of each other clumping together. The most striking result in this figure is that the spike for  $r_0 \sim r_{cr}$  is significantly taller than all the others, and the clustering remains higher for this case even at later times. We shall present further evidence below to show that the annular region close to the critical radius is the most important for clustering.

In figure 5 (b), we show density profiles as a function of radius at a time of  $t = 15\tau$  and  $t = 20\tau$ . By this time, caustics have formed and the participating particles have since dispersed. In this and following figures, when we allude to "only caustics" or "excluding caustics", we refer to initial particle locations  $r_o < 0.8r_{cr}$  and  $r_o > 1.2r_{cr}$  respectively. The values 0.8 and 1.2 have been chosen arbitrarily, and the answers do not change qualitatively when we choose other limits. We refer to initial locations within  $0.8r_{cr} \leq r_o < 1.2r_{cr}$  as the annular region, which will be shown to contribute significantly to the densest regions. To identify where particles originated from, different symbols are given in this figure to the contributions of each of these. We see that there is a minimum radius below which there are no particles, i.e., the density is zero. This minimum radius increases slowly with time, at the rate of  $1/x^3$ . We now discuss the large  $r$  portion of this figure. It is interesting to note that at a given radial location, two possible values of density are seen. This is because every radial location contains one set of particles which started at  $r_i < r_{cr}$  and another which started at  $r_o > r_{cr}$ . Particles that start close to the vortex are thrown out so violently that they reach locations far away from the vortex. Their radial locations are now distributed over a much large radius. On the other hand, particles which started at  $r_o \gg r_{cr}$  have moved much less and display a local density only slightly different from its initial value. Thus the neighbourhoods of caustics and non-caustics particles are of low and high density respectively. The picture changes at lower  $r$ . Here, the densest neighbourhoods are of the parcels which started out in the annular region near  $r_{cr}$ .

## IV. GAUSSIAN VORTICES

Viscosity acts on point vortices by smearing them out into Gaussian vortices. We therefore study how caustics form around Gaussian vortices. We do this by working with Gaussian vortices of fixed maximum vorticities and widths, such that their total strength is the same as for the point vortices. The simulations presented here are inviscid. Figures 6 plot the caustics boundary for the zero inertia and zero velocity initial conditions. We find that caustics are still created by particles initially within the region given by the same critical radius as with point vortices. However, particles which start out very close to the centre of the vortex do not participate in caustics formation in this case, so there is a minimum initial separation of vortex centre and particle for caustics formation. This radius is dependent on the Stokes number of the particles. This is because the effective value of the exponent  $p$  in eq. 2 varies with radius for a Gaussian vortex. Notice that the independence from particle inertia  $\tau$  of equations (8) and (9) is only valid for point vortices, i.e., when  $p = 2$ . For  $p$  values which are lower, we have made computations which show that the results are Stokes number dependent, and below a particular  $p$  for a given  $\tau$ , caustics cannot form. For any  $\tau$ , caustics form only over a range of  $r_0$  between  $1.2 r_v$  and  $r_{cr}$ , where  $r_v$  is the characteristic radius of a Gaussian vortex, defined by

$$\omega(r) = \omega_v e^{-r^2/r_v^2}, \quad (10)$$

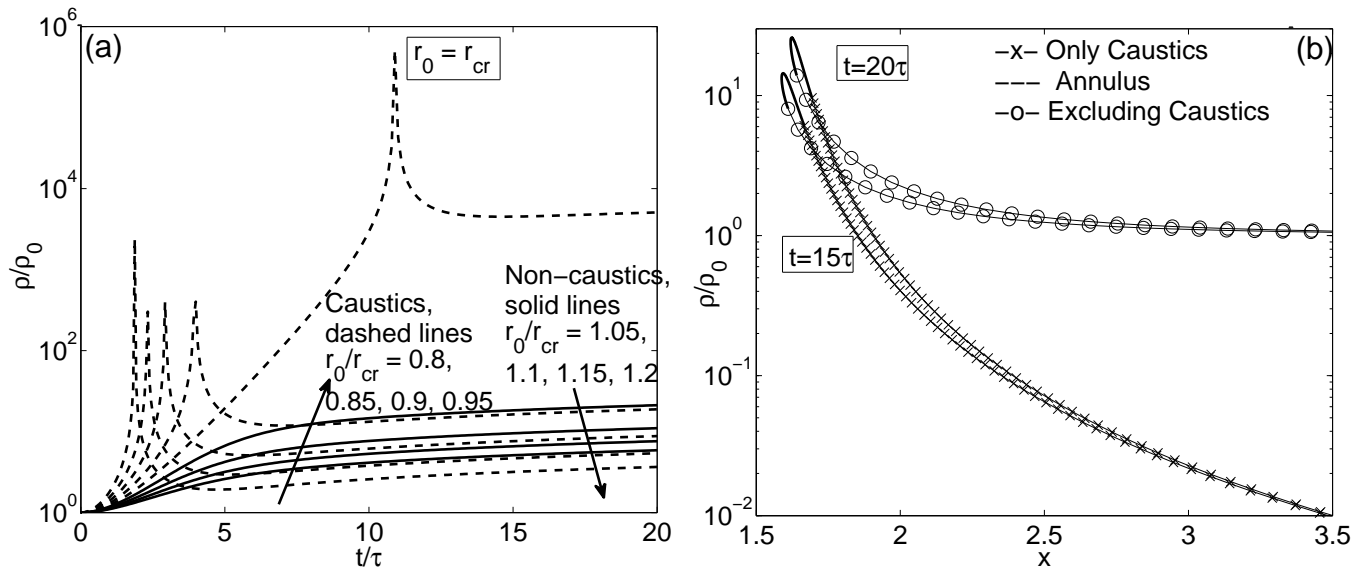


Figure 5: Lagrangian densities for initially co-rotating particles around a single point vortex at the origin. The densities were tracked using the method of Osipov (eq. 14). (a): Density as a function of time for different initial location  $r_0$ . The caustics-producing initial conditions show sharp spikes. (b): Particle density as a function of radial distance from the vortex at  $t = 15\tau$  and  $t = 20\tau$ . There are two possible densities at each radial location, one in the vicinity of particles which started within the caustics-producing region and the other in the neighborhood of particles which started outside this region.

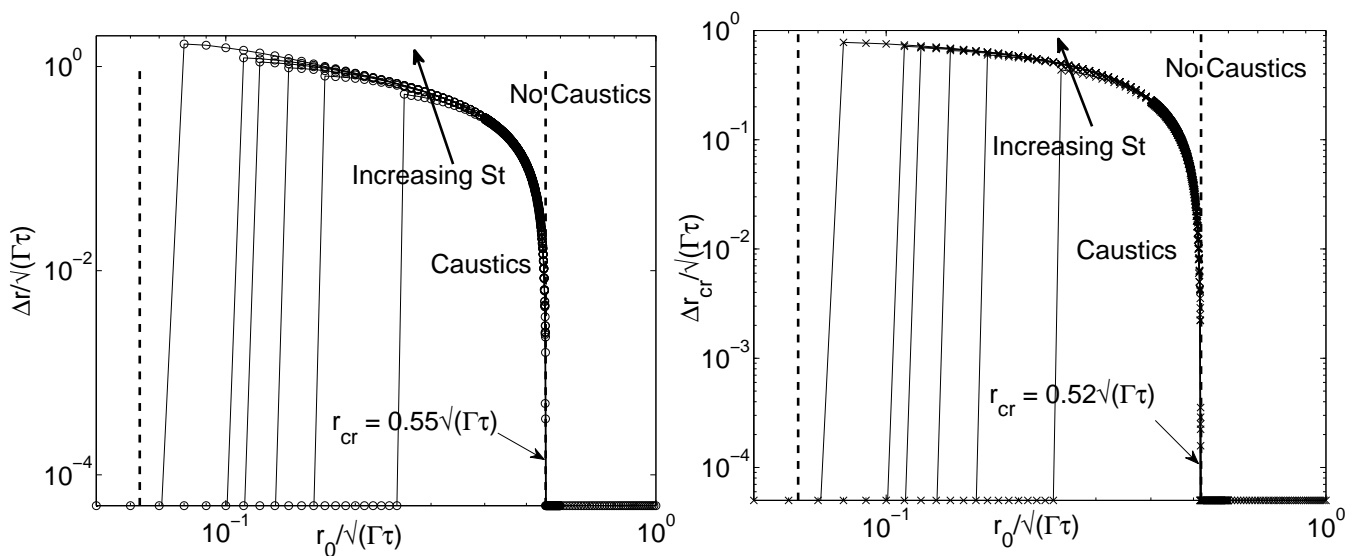


Figure 6: Caustics with Gaussian vortices. These plots are analogous to the plots in figure 4. The maximum vorticity and characteristic radius are the same for all plotted curves. The dashed lines to the left of the curves show the characteristic radius of the Gaussian vortex normalised by the largest inertia. Caustics exist only for  $r_{cr} > r_0 > 1.2 r_v$ , and the inner limit is dependent on  $St$  (see text for a definition of  $St$ ). Left: zero-inertia initial condition, right: zero-velocity. The values of  $St$  shown are 0.04, 0.08, 0.12, 0.16, 0.2 and 0.4.

$\omega_v$  being the peak vorticity. The angular velocity of a particle around the origin is therefore given by

$$\Omega(r) = \int_0^r 2\pi r \omega dr = \frac{\pi \omega_v r_v^2}{2} \left(1 - e^{-r^2/r_v^2}\right) = \frac{\Gamma}{2} \left(1 - e^{-r^2/r_v^2}\right). \quad (11)$$

The  $\Gamma (= \pi \omega_v r_v^2)$  in equation 11 is strength of the Gaussian vortex. Figures 6 show that the vortex strength plays much the same part for Gaussian vortices as it does for point vortices. The Stokes number of a particle may then be



defined using the characteristic radius of the vortex:

$$St = \frac{\Gamma\tau}{r_v^2} \quad (12)$$

Figures 6 plot the analogues of figure 4. The actual value of  $r_v$  does not make a difference to critical radius  $r_{cr}$ . However, the nondimensional parameter  $\omega_v\tau$  (which is a multiple of the particle Stokes number and hence depends on  $r_v$ ) limits the occurrence of caustics. No caustics occur for  $\omega_v\tau \lesssim 4$ . Therefore, as the width  $r_v$  of a Gaussian vortex increases in time due to viscosity, only particles of larger inertia can undergo caustics at later times.

## V. SEVERAL VORTICES

We now apply the same density tracking procedure as in sections III and IV to a system of particles in the flow of several point vortices in a periodic box. The system of point vortices is for us a proxy for two-dimensional turbulence. (While Gaussian vortices would have been more realistic, no expression exists of the form 13 for Gaussian vortices in a periodic box.)

We perform simulations with  $N = 10$  point vortices of the same circulation but random signs (zero net circulation) in a doubly periodic box. The motion of the vortices is computed using the Hamiltonian for this problem [26]:

$$\mathcal{H} = -\frac{1}{2\pi} \sum_{j < k} \Gamma_j \Gamma_k \left[ \ln \left| \vartheta \left( \frac{z_{jk}}{L_x} \right) \right| - \frac{\pi}{\Delta} (\text{Im}(z_{jk}))^2 \right], \quad (13)$$

where  $z_j$  is the position of the  $j$ th vortex in the complex plane:  $z_j = x_j + iy_j$ ;  $L_x$  is the length of the box along the x-direction and  $\Delta = L_x L_y$  is the area of the box.

We study statistics of the particle density as a way of quantifying the effects of caustics in such systems. We perform simulations of three types: (i) by distributing particles at random but removing all particles inside the caustic-producing region of each vortex. In simulations of type (ii) we do the reverse, i.e., only keep particles within the critical  $r_{cr}$  for caustics formation. In simulations of type (iii), we start particles in the annular region  $0.8r_{cr} \leq r \leq 1.2r_{cr}$ . Simulations excluding caustics are done with  $4 \times 10^4$  particles; and simulations with particles only in the caustic regions, and particles in an annulus are done with  $10^4$  particles each. We hold  $\tau$  constant during each simulation. Figure 7 shows particle density in the domain at different times, for initial particle locations exclusively within, and strictly outside, the caustics-forming region, i.e., for particle distributions corresponding to (i) and (ii) above. We notice that the highest densities occur in both cases in the same regions. These appear to correspond to initial conditions at the edge of the caustics-forming region, i.e., around the critical radius. To confirm this, we perform simulations of type (iii). Figures 8 show how significant the region around the critical radius is for producing high density particles, in comparison to the regions well inside and well outside. We also note that the effects of the critical annulus region are more pronounced for the smaller of the two inertia values.

Another point of interest is that there appear to be, in figure 7, "voids" in the distribution of particles in space, with the radius of the voids given by the critical radius. It is known from simulations of two- and three-dimensional turbulence [2, 27] that such voids exist. It is also known that, for small inertia, the voids increase in size with increasing inertia. It is subject to future confirmation whether our idea of a critical radius  $r_{cr}$  for inertial particle caustics is directly connected to these voids (and the dependence of their size on particles inertia). The fact that caustics formation is much faster than flow time-scales, and that a given particle inertia leads to a characteristic void size lends credence to this.

The number of particles with greater than a threshold density, as figure 9 shows (we have checked that the exact value of the threshold does not matter; for this figure a value of 1000 was used) is also much higher for particles starting in the annulus. In fact for the smaller of the two inertias, almost all 'caustic events' happen for particles starting in the annulus.

We plot the distribution of Lagrangian densities for the many-vortex simulations. The plots for particles starting in the 'only caustics' and 'excluding caustics' corroborate the results from section III, figure 5: particles starting outside the caustics region show a monotonically increasing density in their vicinity, whereas particles starting close to vortices get thrown out violently and so a peak in the distribution is seen at very small density. In figure 10, we plot the density distributions for particles starting in the annulus regions for two different values of particle inertia. The curves are plotted at the same advection time (for identical fluid flows, since the particles don't affect the flow), which is a different multiple of each different inertia. The curves show the smaller of the two inertias reaching a higher average density at the same advection time, which is expected, since the heavier particles have had less time in units of  $\tau$  to cluster.



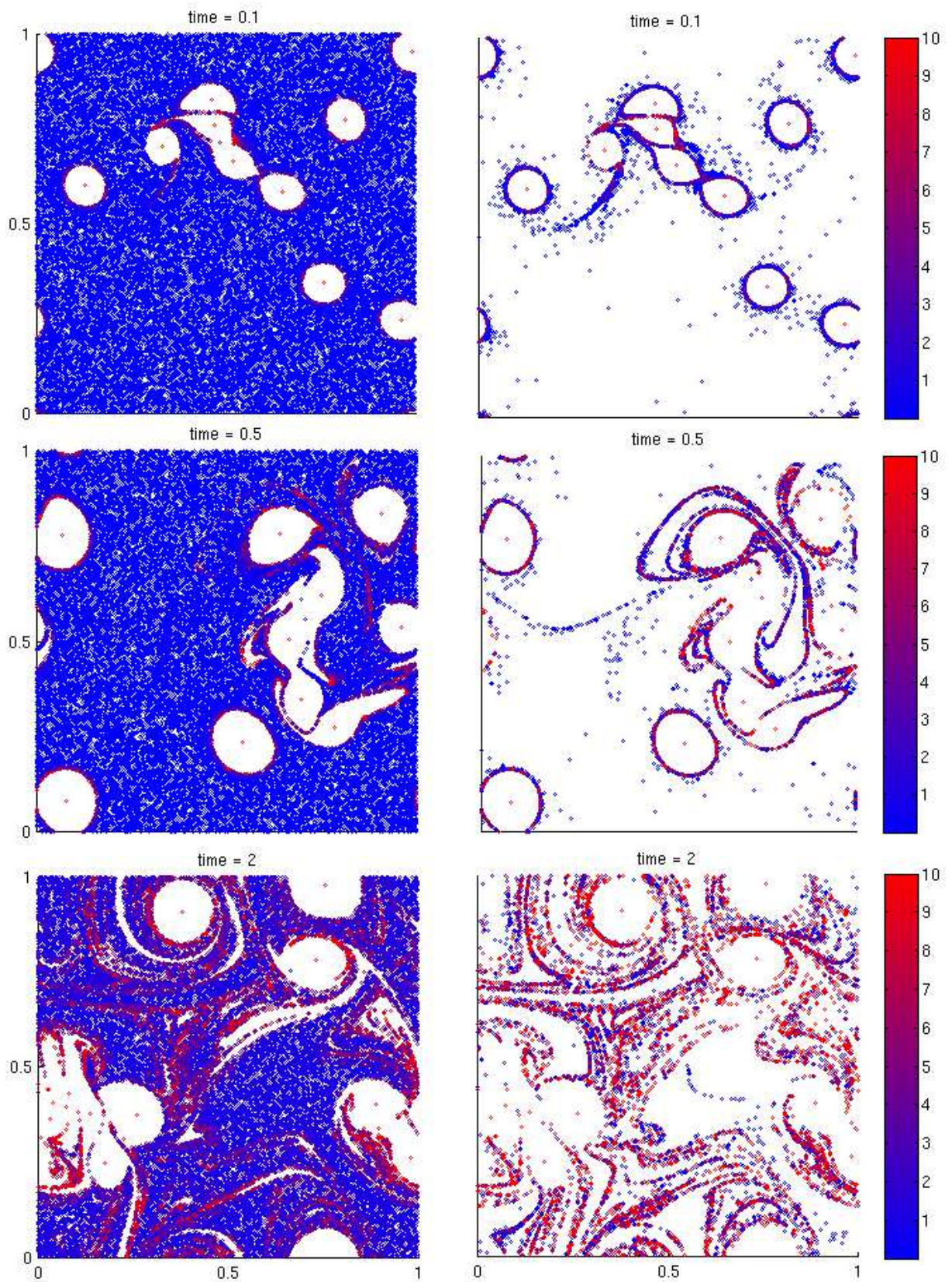


Figure 7: Snapshots at time  $t = 200\tau$  of particle positions with 10 vortices in a doubly periodic  $10 \times 10$  box. The colour indicates local particle density. The particles have  $\tau = 0.001$ . Left: Caustics excluded; right: Only caustics.

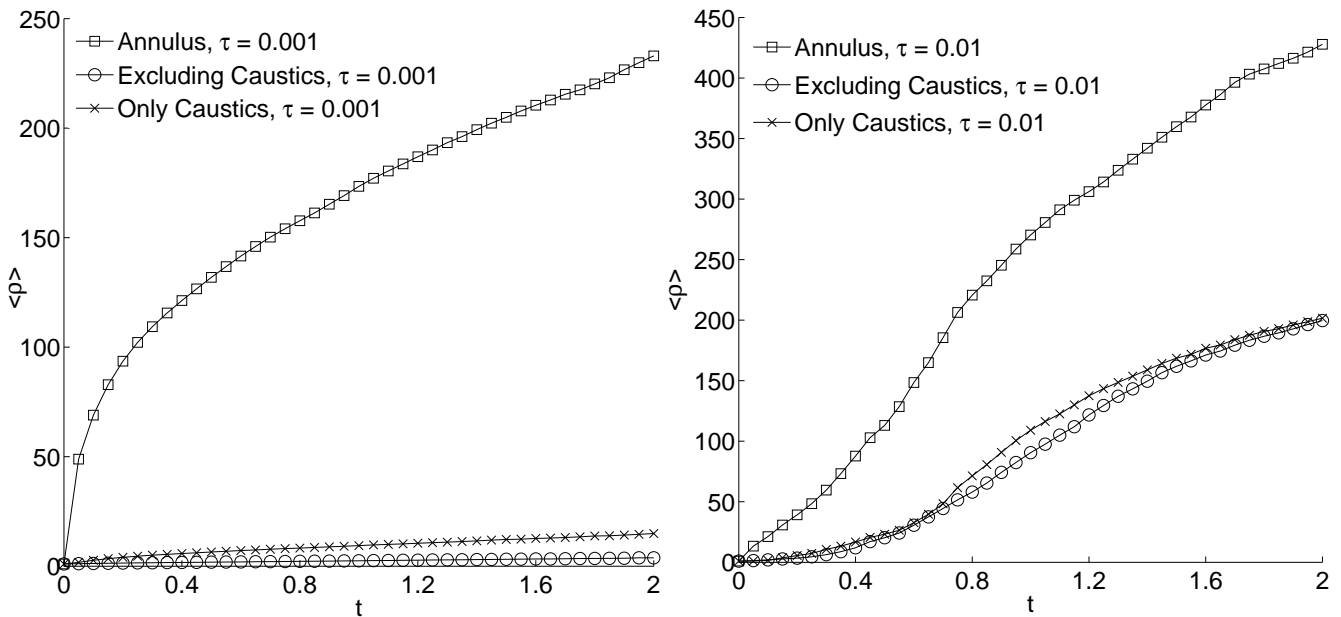


Figure 8: Average Lagrangian densities. The three curves in each plot correspond to particles starting well within, well outside, and in the annulus around the critical radius  $r_{cr}$ . Particles starting close to  $r_{cr}$  are the primary contributors of high density regions. Left:  $\tau = 0.001$ , Right:  $\tau = 0.01$

## VI. CONCLUSION

To summarise, we have studied the formation of caustics in model two-dimensional vortical flows. For a single vortex, we show that only particles which are initially within a critical radius  $r_{cr} \sim 0.5(\Gamma\tau)^{1/2}$  from its centre can cause caustics to form. For a point vortex, particles placed inside this critical radius can only overtake rings of neighbouring particle rings which lie within some initial separation  $(\Delta r)_{cr}$ . The time for such overtaking is the caustics formation time  $T_{caustics}$ . This quantity diverges for  $r_0 \rightarrow r_{cr}$ . The initial separation within which caustics form depend on initial conditions and so does the formation time.

The formation of caustics is intimately related to the creation of regions of high particle density. Our adoption of Osipov's method enables us to track densities in the neighbourhood of Lagrangian particles. Interestingly, particles which lie close to the critical radius, i.e. on the edge of the caustics-producing region, give rise to the largest spikes in density, suggesting that this region should contribute to the effects that particle caustics have on the flow. Indeed, we find that for small inertia, almost all the instances of very dense clusters come from the annular region. In these regions particle collision frequency is likely to be the highest. Further studies are needed to confirm this prediction. Outside the critical radius, particle density displays a qualitatively different behaviour. Density increase is gentle and monotonic in this case for all time.

Our results above show that the centrifugal force can only create caustics in a small area around a vortex. We also show that the biggest density spikes happen not for particles that start well within the caustic regions, but rather for particles that start on the edge of the caustic regions (i.e. for particles which may be considered to have Stokes numbers of order 1). We find also that the effects of this annular region around the critical radius are more prominent for the smaller of the two inertias.

Our results predict that particle collisions in flows with strong vortices are more probable at a critical radius from the vortex. Our future work will test this prediction with more realistic flows than a system point vortices. Whether the existence of this annular band depends on the confinement offered by the two-dimensional nature of our setup is also worth checking. We hope that our work will motivate viscous three-dimensional simulations to check our predictions on the importance of the critical annular region about each vortex in the creation of the densest clusters. In particular it would be useful to ask whether the extent of clustering can be directly correlated to suitably weighted summations of square roots of instantaneous circulations in the flow.

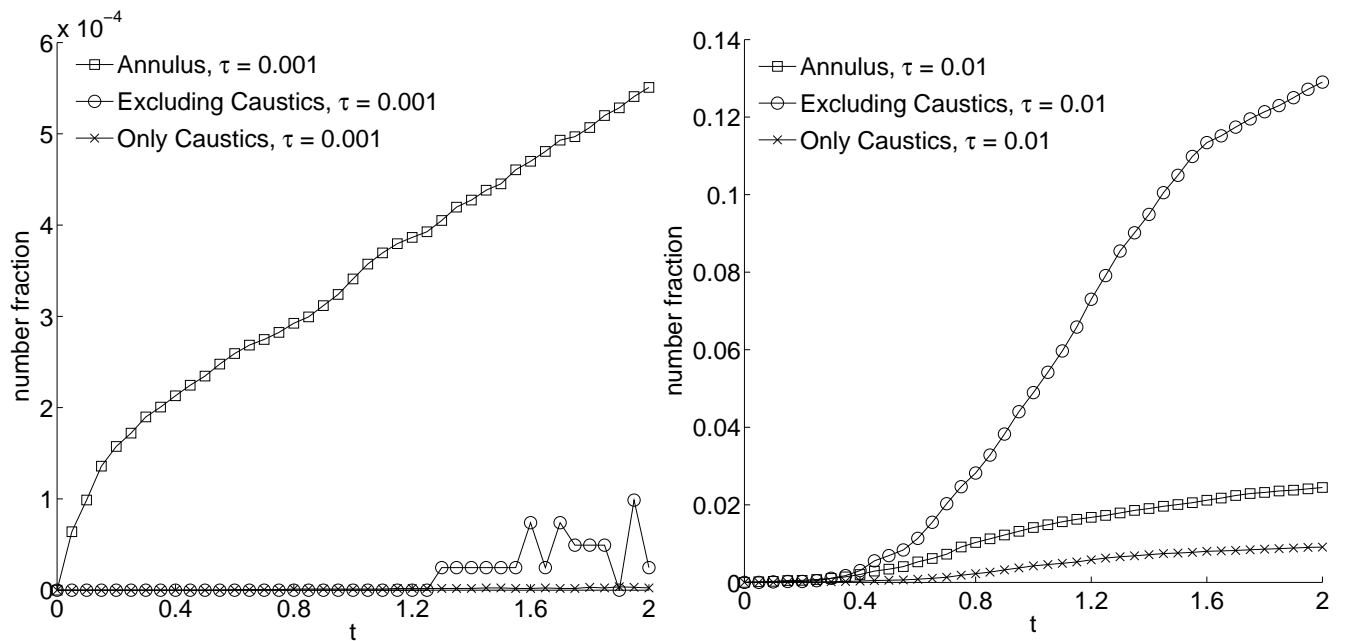


Figure 9: Fraction of particles in high-density regions. We plot the fraction of particles whose neighbourhoods have density greater than a certain threshold, here prescribed to be  $\rho_{cutoff} = 1000\rho_0$ , where  $\rho_0$  is the uniform initial density. Left:  $\tau = 0.001$ , Right:  $\tau = 0.01$ .

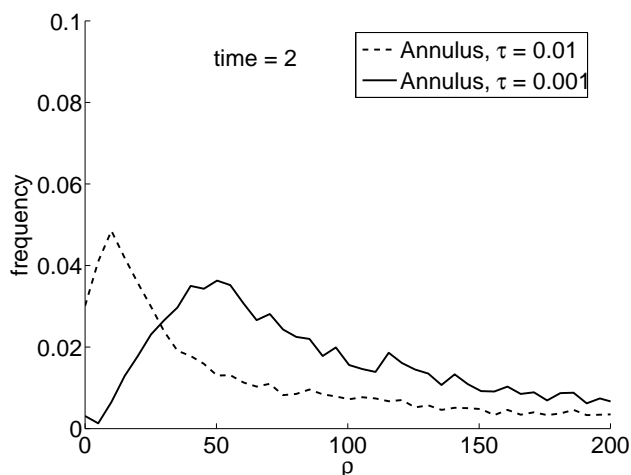


Figure 10: The density distribution for particles starting in the annulus regions for two different values for inertia. The curves for the larger inertia seem to shift towards lower density values.

### Acknowledgements

We thank Raymond Shaw, who suggested we study caustics using our system of point vortices. We thank Nick Ouelette and Jeremie Bec, discussions with whom led to the discussion of voids in particle distribution in section V. We also thank the two referees whose suggestions led among other things to the detailed physical scaling arguments in section III, and a discussion of the validity of the Lagrangian density tracking algorithm in the appendix. This work is partially supported by the Ministry of Earth Sciences, Government of India, under the Monsoon Mission Project on the Bay of Bengal.

### Appendix: Lagrangian Density tracking



The density tracking equations of Healy & Young [23] are modified for a cylindrical polar coordinate system. We follow the same notation as them. They are

$$\begin{aligned}
J_{rr} &= \frac{\partial r}{\partial r_0} \\
w_{rr} &= \frac{\partial J_{rr}}{\partial t_p} = \frac{\partial v_r}{\partial r_0} \\
\frac{\partial w_{rr}}{\partial t_p} &= \frac{\partial}{\partial r_0} \frac{\partial v_r}{\partial t_p} = \frac{\partial}{\partial r_0} \left( -\frac{v_r}{\tau} + r\omega^2 \right) = -\frac{w_{rr}}{\tau} + J_{rr}\omega^2 + 2\omega r w_{\theta r} \\
J_{\theta r} &= \frac{\partial \theta}{\partial r_0} \\
w_{\theta r} &= \frac{\partial \omega}{\partial r_0} \\
\frac{\partial w_{\theta r}}{\partial t_p} &= \frac{\partial}{\partial r_0} \frac{\partial \omega}{\partial t_p} = \frac{\partial}{\partial r_0} \left( \frac{\Omega - \omega}{\tau} - 2\frac{v_r \omega}{r} \right) = \frac{1}{\tau} \left( \frac{\partial \Omega}{\partial r} J_{rr} - w_{\theta r} \right) - 2 \left( \frac{\omega}{r} w_{rr} + \frac{v_r}{r} w_{\theta r} - \frac{v_r \omega}{r^2} J_{rr} \right) \quad (14)
\end{aligned}$$

The equations 14 can be integrated in time to find the density given by

$$\begin{aligned}
J &= |r J_{rr} J_{\theta\theta} - J_{\theta r} J_{r\theta}| = |r J_{rr}| \\
\rho_p &= \frac{\rho_{p,0} r_0}{J}. \quad (15)
\end{aligned}$$

The first of equations 15 includes the factor  $r$  because of the Jacobian involved in transforming from Cartesian to polar coordinates.

**A comment on the validity of Lagrangian density tracking** Osipov's method as described above calculates the density around a particle as it moves along on its trajectory, and does this without reference to how many other particles are around the particle being tracked. We have found that Lagrangian density tracking is better than the usual way of calculating density (which is to count the number of particles per unit area/volume). However, the density predicted by the method will only be realised in a real flow if there is in fact a continuum of particles that converge onto (or diverge away from) the particle being tracked. Since this is hardly observed in real flows (in clouds, for example, there is on average one particle per every few Kolmogorov boxes), the answers from Osipov's method must be taken with a pinch of salt.

- 
- [1] Bec, J. (2003). Fractal clustering of inertial particles in random flows. *Physics of Fluids*, 15(11), L81. doi:10.1063/1.1612500
  - [2] Bec, J., Biferale, L., Cencini, M., Lanotte, A., Musacchio, S., & Toschi, F. (2007). Heavy particle concentration in turbulence at dissipative and inertial scales. *Physical Review Letters*, 98(8), 084502.
  - [3] Bec, J., Celani, A., Cencini, M., & Musacchio, S. (2005). Clustering and collisions of heavy particles in random smooth flows. *Physics of Fluids*, 17(7), 073301. doi:10.1063/1.1940367
  - [4] J. K. Eaton and J. R. Fessler, (1994). Preferential concentration of particles by turbulence. *Int. J. Multiphase Flow*, 20, 169.
  - [5] Shaw, R. A., Reade, W. C., Collins, L. R., & Verlinde, J. (1998). Preferential concentration of cloud droplets by turbulence: Effects on the early evolution of cumulus cloud droplet spectra. *Journal of the Atmospheric Sciences*, 55(1993), 1965–1976.
  - [6] Chen, L., Goto, S., & Vassilicos, J. C. (2006). Turbulent clustering of stagnation points and inertial particles. *Journal of Fluid Mechanics*, 553(-1), 143. doi:10.1017/S0022112006009177
  - [7] Gibert, M., Xu, H., & Bodenschatz, E. (2012). Where do small, weakly inertial particles go in a turbulent flow? *Journal of Fluid Mechanics*, 698, 160–167. doi:10.1017/jfm.2012.72
  - [8] Goto, S., & Vassilicos, J. (2008). Sweep-Stick Mechanism of Heavy Particle Clustering in Fluid Turbulence. *Physical Review Letters*, 100(5), 1–4. doi:10.1103/PhysRevLett.100.054503
  - [9] Sapsis, T., & Haller, G. (2010). Clustering criterion for inertial particles in two-dimensional time-periodic and three-dimensional steady flows. *Chaos*, 017515(2010), 11. doi:10.1063/1.3272711
  - [10] M. R. Maxey (1987). The gravitational settling of aerosol particles in homogeneous turbulence and random flow fields. *Journal of Fluid Mechanics*, 174, pp 441-465 doi:10.1017/S0022112087000193
  - [11] Wilkinson, M., & Mehlig, B. (2005). Caustics in turbulent aerosols. *Europhysics Letters (EPL)*, 71(2), 186–192. doi:10.1209/epl/i2004-10532-7
  - [12] Duncan, K., Mehlig, B., Ostlund, S., & Wilkinson, M. (2005). Clustering by Mixing Flows. *Physical Review Letters*, 95(24), 240602. doi:10.1103/PhysRevLett.95.240602
  - [13] Wilkinson, M., Mehlig, B., & Bezuglyy, V. (2006). Caustic Activation of Rain Showers. *Physical Review Letters*, 97(4), 048501. doi:10.1103/PhysRevLett.97.048501

- [14] Mehlig, B., Uski, V., & Wilkinson, M. (2007). Colliding particles in highly turbulent flows. *Physics of Fluids*, 19(9), 098107. doi:10.1063/1.2768931
- [15] Wilkinson, M., Mehlig, B., & Gustavsson, K. (2010). Correlation dimension of inertial particles in random flows. *EPL (Europhysics Letters)*, 89(5), 50002. doi:10.1209/0295-5075/89/50002
- [16] Gustavsson, K., & Mehlig, B. (2011). Ergodic and non-ergodic clustering of inertial particles. *EPL (Europhysics Letters)*, 96(6), 60012. doi:10.1209/0295-5075/96/60012
- [17] Gustavsson, K., Meneguz, E., Reeks, M., & Mehlig, B. (2012). Inertial-particle dynamics in turbulent flows: caustics, concentration fluctuations and random uncorrelated motion. *New Journal of Physics*, 14(11), 115017. doi:10.1088/1367-2630/14/11/115017
- [18] Gustavsson, K., & Mehlig, B. (2013). Distribution of velocity gradients and rate of caustic formation in turbulent aerosols at finite Kubo numbers. *Physical Review E*, 87(2), 023016. doi:10.1103/PhysRevE.87.023016
- [19] Falkovich, G., & Pumir, A. (2007). Sling Effect in Collisions of Water Droplets in Turbulent Clouds. *Journal of the Atmospheric Sciences*, 64(12), 4497–4505. doi:10.1175/2007JAS2371.1
- [20] Falkovich, G., Fouxon, A., & Stepanov, M. G. (2002). Acceleration of rain initiation by cloud turbulence. *Nature*, 419(9), 151–154. doi:10.1038/nature00985.1
- [21] Raju, N., & Meiburg, E. (1997). Dynamics of small, spherical particles in vortical and stagnation point flow fields. *Physics of Fluids*, 9(February), 299–314.
- [22] Maxey, M. R., & Riley, J. J. (1983). Equation of motion for a small rigid sphere in a nonuniform flow. *Physics of Fluids*, 26(4), 883. doi:10.1063/1.864230
- [23] Healy, D. P., & Young, J. B. (2005). Full Lagrangian methods for calculating particle concentration fields in dilute gas-particle flows. *Proceedings of the Royal Society A: Mathematical, Physical and Engineering Sciences*, 461(2059), 2197–2225. doi:10.1098/rspa.2004.1413
- [24] IJzermans, R., Reeks, M., Meneguz, E., Picciotto, M., & Soldati, a. (2009). Measuring segregation of inertial particles in turbulence by a full Lagrangian approach. *Physical Review E*, 80(1), 015302. doi:10.1103/PhysRevE.80.015302
- [25] Meneguz E., Reeks M. & Soldati A., (2009), Quantification of heavy particle segregation in turbulent flows: a lagrangian approach, *Chemical Engineering Transactions*, 17, 537-542. doi:10.3303/CET0917090
- [26] O’Neil, K. a. (1989). On the Hamiltonian dynamics of vortex lattices. *Journal of Mathematical Physics*, 30(6), 1373. doi:10.1063/1.528605
- [27] Boffetta, G., De Lillo, F., & Gamba, A. (2004). Large scale inhomogeneity of inertial particles in turbulent flows. *Physics of Fluids*, 16(4), L20-L23.